Inorg. Chem. **2003**, *42*, 7162–7172

How Strong Can the Bend Be on a DNA Helix from Cisplatin? DFT and MP2 Quantum Chemical Calculations of Cisplatin-Bridged DNA Purine Bases

Jaroslav V. Burda*,† and Jerzy Leszczynski‡

Department of Chemical Physics and Optics, Faculty of Mathematics and Physics, Charles University, Ke Karlovu 3, 121 16 Prague 2, Czech Republic, and Department of Chemistry, Jackson State University, 1325 J.R. Lynch Street, Jackson, Mississippi 39217-0510

Received March 18, 2003

The B3LYP/6-31G(d) level of theory was used for the optimization of $[Pt(NH_3)_4]^{2+}$, $[Pt(NH_3)_3(H_2O)]^{2+}$, *cis*-$[Pt(NH_3)_2(H_2O)_2]^{2+}$, and related platinum complexes. In addition, water or ammonium ligands were replaced by DNA purine bases so that finally *cis*-diammineplatinum with two bases (Pt-bridged complexes) is obtained. Single point calculations using the MP2/6-31+G(d) method were performed on the obtained reference geometries and were utilized for estimating bond dissociation energies (BDEs) and stabilization energies, and for electron density analyses. After reoptimization, IR spectra were determined from HF second derivatives. It was found that replacement of both water and ammonium by the DNA base is an exothermic process (20–50 kcal/mol depending on the ligands present in the complex). Asymmetric structures with one interbase H-bond were obtained for *cis*-diammine–(N_7,N_7'-diadenine)–platinum and mixed *cis*-diammine–(N_7-adenine)–(N_7-guanine)–platinum complexes. In the case of the diguanine Pt-bridge, a symmetrical complex with two ammonium$\cdots O_6$ H-bonds was found. The higher stabilization energy of the di-guanine complex is linked to a larger component of the Coulombic interaction. However, the BDE of Pt–N_7(G) is smaller in this complex than the BDE of Pt–N_7(G) from the mixed Pt–AG complex. Also, steric repulsion of the ligands is about 10 kcal/mol smaller for the asymmetrical Pt–AA and Pt–AG bridges. The influence of the trans effect on DBE can be clearly seen. Adenine exhibits the largest trans effect, followed by guanine, ammonium, and water. The strength of the H-bond can be determined from the IR spectra. The strongest H-bond is the interbase H-bridge between adenine and guanine in the mixed Pt–AG complex; otherwise, the H-bonds of adenine complexes are weaker than in guanine complexes. BDE can be traced in the guanine-containing complexes. The nature of the covalent bonding is analyzed in terms of partial charges and MO. A general explanation of the lower affinity of transition metals to oxygen than nitrogen can be partially seen in the less favorable geometrical orientation of lone electron pairs of oxygen.

Introduction

After the discovery of the anticancer activity of cisplatin by Rosenberg,[1] a great deal of attention was drawn to platinum compounds of both Pt(II) and Pt(IV). Toward the end of 1980s, a second generation of cisplatin analogues appeared of which carboplatin has proven to be one of the most useful.[2] These exhibit equivalent therapeutic effects as compared to that of cisplatin with lower required doses and thus reduced side effects. One of the first crystal structures of a DNA oligomer with cisplatin was solved in the Dickerson group with resolution of 2.6 Å.[3] A similar structure of triammineplatinum adduct appeared also later.[4] In the same year, a cisplatin G−Pt−G bridge[5] was described also with a resolution of 2.6 Å. An interstrand cisplatin bridge[6] was

* To whom correspondence should be addressed. E-mail: burda@karlov.mff.cuni.cz.
† Charles University.
‡ Jackson State University.

(1) Rosenberg, B.; Van Camp, L.; Trosko, J. L.; Mansour, V. H. *Nature* **1969**, *222*, 385.
(2) Kaim, W.; Schwederski, B. *Bioinorganic Chemistry: Inorganic Elements in the Chemistry of Life*; John Wiley & Sons Ltd: Chichester, England, 1994.
(3) Wing, R. M.; Pjura, P.; Drew, H. R.; Dickerson, R. E. *EMBO J.* **1984**, *3*, 1201.
(4) Parkinson, G. N.; Arvantis, G. M.; Lessinger, L.; Ginell, S. L.; Jones, R.; Gaffney, B.; Berman, H. M. *Biochemistry* **1995**, *34*, 15487.

10.1021/ic034296w CCC: $25.00
Published on Web 10/01/2003

found in excellent resolution, 1.63 Å. Recently, also an oxaliplatin 1,2-d(GpG) intrastrand cross-link in a DNA oligomer was published[7] as was the asymmetric platinum complex $[Pt(ammine)(cyclohexylamine)]^{2+}$ bound to a dodecamer DNA duplex,[8] both at a resolution of 2.4 Å.

Recently, a variety of six-coordinate platinum(IV) complexes were explored as third generation drugs. These complexes are stable enough and can pass through the digestive tract. After absorption into the bloodstream, these compounds are metabolized and form four-coordinate Pt(II) cisplatin analogues.[9] Such drugs were developed on the basis of a much deeper understanding of platinum(II) interactions with DNA; e.g., in the Lippard group, the crystal structure of cisplatin−DNA oligomer−HMG protein was successfully solved.[10,11] Some models of the distortion of DNA after the addition of cisplatin were published already by Lilley.[12] A summary of the current state in the treatment of platinum drugs was completed by Wong.[13] Also, Reedijk[14] revealed some new aspects of competition between S-donor ligands and DNA.[15] The binding properties of quarternary platinum complexes in solution were examined by Sigel and Lippert,[16] and a comparison of platinum−guanine complexes with other selected metal−guanine cations was published.[17] An important problem of the reaction rates was explored in a number of works.[18,19] The structural aspects of platinum interstrand cross-linked binding to DNA bases was also studied in detail by Brabec.[20] In work from the Marzilli group,[21] several conformers of the cisplatin adduct to GpG were examined with different phosphodiester backbones and guanine orientations using NMR (^1H and ^{31}P), CD spectroscopy, and MM and MD calculations.

Many theoretical studies have appeared that were intended to support experimental measurements and to add some detailed insight at the molecular level. Interactions of cisplatin with the 1,2-d(GpG) sequence were examined by Carloni.[22] Here, some hydration aspects of cisplatin are described using Car−Parrinello MD simulations. Comprehensive data on the thermodynamics of hydration can be also found in our studies.[23,24] The DFT method was used in a study by Wysokinski[25] for a comparison of the structure and vibrational spectra of cisplatin and carboplatin. A comprehensive analysis of the conformers of DDP was performed in a study by Pavankumar.[26] The stabilization of rare tautomers and the possibility of mispairs in DNA due to N_4 platinated cytosine were explored by Šponer[27] and due to N_7-platinated guanine and adenine by Burda.[28,29] Chval studied the transition state in the chloride ligand replacement with water and guanine.[30]

From a computational point of view, an interesting review of the nature of bonding in transition metal complexes was published by Frenking.[31] Here, some general features that are important in platinum complexes were analyzed. Also, the IMOMM/ONIOM method was applied to Pt complexes and seems to be a useful approach for examining larger structures.[32]

Force field parameters for platinum were developed by Cundari[33] that could enable classical molecular simulation of extended molecular systems. Recent work of Deubel[34] compares the cisplatin affinity of various S-sites and N-sites from amino acids with purine DNA bases. DFT techniques were used with the VTZP basis set, and relevant results are in excellent accord with our data. The influence of Pt coordination on the N_7 site of purine on the strength of the N_9-C_1' glycosyl bond is solved in a theoretical study from the Lippard group.[35]

Despite the differences in various generations of cisplatin analogues, there are some common features related to the Pt(II) binding to DNA chains. It was found that the most abundant and key complex involves two guanines bridged by Pt(II)−1,2-d(GpG) or less frequently also 1,3-d(GpXpG). Also, other intrastrand coordination occurs, namely, diammine−(N_7-adenine)−(N_7-guanine)−platinum from the 1,2-d(ApG) DNA−cisplatin complexes (usually, not from 1,2-d(GpA) DNA adduct), but diammine−(N_7,N_7'-diadenine)−

(5) Takahara, P. M.; Rosenzweig, A. C.; Frederick, C. A.; Lippard, S. J. *Nature* **1995**, *377*, 649.
(6) Coste, F.; Malinge, J. M.; Serre, L.; Shepard, W.; Roth, M.; Leng, M.; Zelwer, C. *Nucleic Acids Res.* **1999**, *27*, 1837.
(7) Spingler, B.; Whittington, D. A.; Lippard, S. J. *Inorg. Chem.* **2001**, *40*, 5596.
(8) Silverman, A. P.; Bu, W.; Cohen, S. M.; Lippard, S. J. *J. Biol. Chem.* **2002**, *277*, 49743.
(9) Kelland, L. R.; Murrer, B. A.; Abel, G.; Giandomenico, C. M.; Mistry, P.; Harrap, K. R. *Cancer Res.* **1992**, *52*, 822−828.
(10) Ohndorf, U.-M.; Rould, M. A.; He, Q.; Pabo, C. O.; Lippard, S. J. *Nature* **1999**, *399*, 708−712.
(11) Jamieson, E. R.; Lippard, S. J. *Chem. Rev.* **1999**, *99*, 2467−2498.
(12) Lilley, D. M. J. *JBIC, J. Biol. Inorg. Chem.* **1996**, *1*, 189−191.
(13) Wong, E.; Giandomenico, C. M. *Chem. Rev.* **1999**, *99*, 2451−2466.
(14) Reedijk, J. *Chem. Commun.* **1996**, *7*, 801−806.
(15) Reedijk, J. *Chem. Rev.* **1999**, *99*, 2499−2510.
(16) Sigel, H.; Song, B.; Oswald, G.; Lippert, B. *Chem. Eur. J.* **1998**, *4*, 1053−1060.
(17) Song, B.; Zhao, J.; Griesser, R.; Meiser, C.; Sigel, H.; Lippert, B. *Chem. Eur. J.* **1999**, *5*, 2374−2387.
(18) Jestin, J.-L.; Lambert, B.; Chottard, J.-C. *JBIC, J. Biol. Inorg. Chem.* **1998**, *3*, 515−519.
(19) Arpalahti, J. In *Metal Ions in Biological Systems*; Sigel, A., S. H., Ed.; Marcel Dekker: New York, 1996; Vol. 32, pp 380−395.
(20) Brabec, V.; Neplechova, K.; Kasparkova, J.; Farell, N. *JBIC, J. Biol. Inorg. Chem.* **2000**, *5*, 364−368.
(21) Williams, K. M.; Scarcia, T.; Natile, G.; Marzilli, L. G. *Inorg. Chem.* **2001**, *40*, 445−454.
(22) Carloni, P.; Sprik, M.; Andreoni, W. *J. Phys. Chem. B* **2000**, *104*, 823−835.
(23) Burda, J. V.; Zeizinger, M.; Sponer, J.; Leszczynski, J. *J. Chem. Phys.* **2000**, *113*, 2224−2232.
(24) Zeizinger, M.; Burda, J. V.; Šponer, J.; Kapsa, V.; Leszczynski, J. *J. Phys. Chem. A* **2001**, *105*, 8086−8092.
(25) Wysokinski, R.; Michalska, D. *J. Comput. Chem.* **2001**, *22*, 901−912.
(26) Pavankumar, P. N.; Seetharamulu, P.; Yao, S.; Saxe, J. D.; Reddy, D. G.; Hausheer, F. H. *J. Comput. Chem.* **1999**, *20*, 365−382.
(27) Šponer, J.; Šponer, J. E.; Gorb, L.; Leszczynski, J.; Lippert, B. *J. Phys. Chem. A* **1999**, *103*, 11406−11413.
(28) Burda, J. V.; Šponer, J.; Leszczynski, J. *JBIC, J. Biol. Inorg. Chem.* **2000**, *5*, 178−188.
(29) Burda, J. V.; Šponer, J.; Leszczynski, J. *Phys. Chem. Chem. Phys.* **2001**, *3*, 4404−4411.
(30) Chval, Z.; Šíp, M. *J.THEOCHEM* **2000**, *532*, 59−68.
(31) Frenking, G.; Froehlich, N. *Chem. Rev.* **2000**, *100*, 717−774.
(32) Svensson, M.; Humbel, S.; Froese, R. D. J.; Matsubara, T.; Sieber, S.; Morokuma, K. *J. Phys. Chem.* **1996**, *100*, 19357−19363.
(33) Cundari, T. R.; Fu, W.; Moody, E. W.; Slavin, L. L.; Snyder, L. A.; Sommerer, S. O.; Klinckman, T. R. *J. Phys. Chem.* **1996**, *100*, 18057−18064.
(34) Deubel, D. V. *J. Am. Chem. Soc.* **2002**, *124*, 5834−5842.
(35) Baik, M.-H.; Friesner, R. A.; Lippard, S. J. *J. Am. Chem. Soc.* **2002**, *124*, 4495−4503.

platinum coordination of 1,2-d(ApA) was observed only very rarely. The main question that we would like to address here concerns the strength of the Pt-bridges in these complexes and their physical description.

Computational Details

Full optimizations of tetraligated Pt(II) square-planar complexes were performed in the frame of the DFT method with the Becke3LYP functional[36] with the 6-31G(d) basis set. All complexes were based on 2+ charged tetraammineplatinum $[Pt(NH_3)_4]^{2+}$ (Pt_a_4), aqua-triammineplatinum $[Pt(NH_3)_3(H_2O)]^{2+}$ (Pt_a_3w), and *cis*-diaqua-diammineplatinum *cis*-$[Pt(NH_3)_2(H_2O)_2]^{2+}$ (Pt_a_2w_2). Concerning diammine−Pt bridges, only one water ligand can be present, at maximum, in the case of single-base complexes. Thus, four $[Pt(NH_3)_2LB]^{2+}$ cations were considered after the first substitution; L labels H_2O or NH_3, and B designates adenine or guanine, namely triammine−(N_7-guanine)−platinum (these two structures were obtained in a previous investigation of the influence of platinum complexes on tautomers of guanine and adenine[28]) (Pt_a_3G), triammine−(N_7-adenine)−platinum[1] (Pt_a_3A), *cis*-diammine−aqua−(N_7-guanine)−platinum (Pt_a_2wG), and *cis*-diammine−aqua−(N_7-adenine)−platinum (Pt_a_2wA). Three complexes were obtained after the second substitution: *cis*-diammine−(N_7,N_7'-diguanine)−platinum (Pt_a_2G_2), *cis*-diammine−(N_7-adenine)−(N_7-guanine)−platinum (Pt_a_2AG), and *cis*-diammine−(N_7,N_7'-diadenine)−platinum (Pt_a_2A_2).

It is known that DFT methods are not capable of correctly describing the dispersion part of the correlation energy. Therefore, the perturbation theory was chosen for scanning changes of stacking energies by comparing two neighboring DNA bases and bases in platinum-bridged complexes. Complex stabilizations, bond dissociation energies, and reaction energies for ligand replacement were computed at the MP2(frozen core)/6-31+G(d) level with inclusion of the basis set superposition error (BSSE) of the Boys−Bernardi counterpoise method.[37] Stuttgart energy-averaged relativistic pseudopotentials[38] were used to describe the Pt atom. Its valence basis set was extended with a set of diffuse functions $\alpha_s = 0.0075$, $\alpha_p = 0.013$, and $\alpha_d = 0.025$, and with optimized polarization functions $\alpha_f = 0.98$.[23]

The stabilization energy is defined as

$$\Delta E^{\mathrm{stab}} = -\Delta E^{\mathrm{inter}} = -[E^{\mathrm{compl}} - \sum E^{\mathrm{parts}}(\mathrm{bsse})] \qquad (1)$$

where E^{parts}(bsse) denotes the individual parts of the complex with ghost functions on the remaining atoms. The complexes were considered to be composed of five species: four ligands and a Pt^{2+} cation. Another modification of the stabilization energy E^{stex}, which excludes the sterical effects of the ligands, is suggested. Instead of a sum of individual ligand energy, the structure of all ligands L_1−L_4 are treated as one part, on the basis of the following complex-optimized structure:

$$\Delta E^{\mathrm{stex}} = \sum_{i=1}^{4} E^{\mathrm{L}_i}(\mathrm{bsse}) - E^{\mathrm{L}_1-\mathrm{L}_4}(\mathrm{bsse})] \qquad (1a)$$

An estimation of bond dissociation energy (BDE) was accomplished according to the following formula:

$$\Delta E = -[E^{\mathrm{compl}} - E^{\mathrm{1stfragment}}(\mathrm{bsse}) - E^{\mathrm{2ndfragment}}(\mathrm{bsse})] \qquad (2)$$

Energies of both fragments are again BSSE-corrected.

Utilizing such a treatment, expected errors should remain under 5 kcal/mol.

From NDB databases (http://ndbserver.rutgers.edu/NDB), selected DNA sequences were chosen[39−41] where stack adenine−adenine, adenine−guanine, and guanine−guanine bases occur. These stacked bases were extracted and refilled with hydrogens. The hydrogen positions were reoptimized using the density functional method (Becke3LYP/6-31G(d)). The final structures were analyzed consistently at the MP2/6-31+G(d) level of theory. Two ways of estimation of the stacking interaction were chosen. The first is "uncorrected" subtraction of total energies of stacked bases and optimized isolated bases, and the second is the calculation with inclusion of BSSE corrections similar to eq 2 for BDE. Here, the geometries of the bases were taken from the optimized complex structure, and BSSE calculations were performed considering ghost functions on the other base.

Since it is well-known that the quality of predicted spectra is acceptable at the HF/6-31G(d) level of computation with some recommended additional scaling, this approximation was chosen for the studied complexes. After geometry reoptimization, the scaling factor of 0.8929 was applied for the estimation of IR spectra.[42]

All calculations were done with quantum chemical program package Gaussian 98.[43]

Results and Discussion

The obtained energies of the examined structures were used for the elucidation of the substitution reactions in the course of interactions of tetraammineplatinum or *cis*-diaqua−diammineplatinum cations with DNA bases, where ligands L_1 and L_2 are water or ammonium (cf. Scheme 1). Such

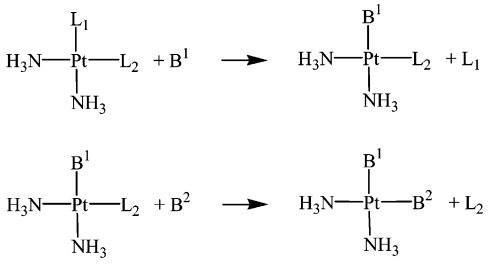

reaction energies are employed in subsequent discussions.

Optimized Geometries. Some important geometry characteristics of the studied structures are compiled in Tables 1 and 2. Table 1 contains Pt−L_x distances and L_1−Pt−L_2 valence angles; the labeling of individual ligands is depicted in Scheme 1. Table 2 further summarizes the detailed features of coordinated bases. First, small complexes of Pt_a_4, Pt_a_3w, and Pt_a_2w_2 were consistently recalculated. Since these

(36) Becke, A. D. In *Modern Electronic Structure Theory*; Yarkoni, Ed.; 1995.
(37) Boys, S. F.; Bernardi, F. *Mol. Phys.* **1970**, *19*, 553−566.
(38) Andrae, D.; Haussermann, U.; Dolg, M.; Stoll, H.; Preuss, H. *Theor. Chim. Acta* **1990**, *77*, 123−141.
(39) Heinemann, U.; Hahn, M. *J. Biol. Chem.* **1992**, *267*, 7332−7341.
(40) Rozenberg, H.; Rabinovich, D.; Frolow, F.; Hegde, R. S.; Shakked, Z. *Proc. Natl. Acad. Sci. U.S.A.* **1998**, *95*, 15194−15199.
(41) Vlieghe, D.; Turkenburg, J. P.; Van Meervelt, L. *Acta Crystallogr., Sect. D* **1999**, *55*, 1495−1502.
(42) Pople, J. A.; Schlegel, H. B.; Krishnan, R.; Defrees, D. J.; Binkley, J. S.; Frish, M. J.; Whiteside, R. A.; Hout, R. F.; Hehre, W. J. *Int. J. Quantum Chem.* **1981**, *15*, 269.

Table 1. Geometry Characteristics of Platinum Complexes[a]

species	L_1	Pt-L_1	L_2	Pt−L_2	L_3	Pt−L_3	L_4	Pt−L_4	L_1−Pt−L_2	L^a−Pt−N_7−C_5	L^a−Pt−N'_7−C'_5
Pt_a_2w_2	a	2.047	a	2.047	w	2.109	w	2.109	93.8		
Pt_a_3w	a	2.087	a	2.055	w	2.109	a	2.097	91.2		
Pt_a_4	a	2.097	a	2.097	a	2.097	a	2.097	90.0		
Pt_a_2wA	A	2.052	a	2.071	w	2.065	a	2.089	91.6	39.4	
Pt_a_3A	A	2.057	a	2.109	a	2.092	a	2.117	90.2	51.5	
Pt_a_2wG	G	2.055	a	2.073	w	2.054	a	2.086	91.5	45.2	
Pt_a_3G	G	2.061	a	2.111	a	2.082	a	2.112	90.0	57.5	
ddl017[b](2.6)	G	2.164	a		a		a				
	G	2.232	a		a		a				
	G	2.315	a		a		a				
zdfb42[c]	G	2.246	a	2.044	a	2.025	a	2.000	91.6	47.59	
	G	2.245	a	2.044	a	2.025	a	1.999	91.6	47.56	
Pt_a_2A_2(s)	A	2.062	A	2.062	a	2.088	a	2.088	94.5	54.3	54.3
Pt_a_2A_2	A	2.048	A	2.045	a	2.091	a	2.099	90.6	51.1	106.8
Pt_a_2AG	A	2.041	G	2.044	a	2.089	a	2.095	91.6	54.5	94.1
Pt_a_2G_2	G	2.065	G	2.065	a	2.074	a	2.074	93.4	60.9	60.9
ddlb73[d] (2.60)	G	1.925	G	1.859	a	1.902	a	1.883	99.5	92.6	142.6
	G	1.914	G	1.901	a	1.916	a	1.890	99.9	93.7	139.4
dd0038[e] (1.63)	G	2.010	G	1.991	a	2.104	a	1.948	86.4	*d*	*d*
dd0040[f] (2.40)	G	1.945	G	1.979	a	2.028	a	2.041	98.4	72.4	143.1
dd0050[g] (2.40)	G	1.961	G	1.961	a	2.014	a	2.045	98.5	74.0	130.4

[a] Pt−L distances (in Å); for ligand notation see scheme 1. L means O atom in water or N atom in ammine ligand L_3 (in Scheme 1). [b] For ddl017, see ref 3, cisplatin coordination to single guanine base in DNA oligomer. The resolution of the database structures is given in parentheses. [c] For zdfb42, see ref 4, contains structure of triammineplatinum adduct to guanine. [d] For ddlb73, see ref 5, major cisplatin adduct with GpG bridge. [e] For dd0038, see ref 6, where guanines have head-to-tail orientation in interstrand cisplatin G−Pt−G bridge. [f] For dd0040, see ref 7, oxaliplatin 1,2-GpG adduct. [g] For dd0050, see ref 8, Pt(ammine)(cyclohexaamine) intrastrand bridge.

Scheme 1. Ligand Ordering[a]

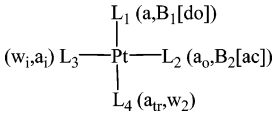

[a] L_1 represents ammine-group or first DNA base, H-bond donating base; L_2 labels noninteracting outer cis-ammine group or second base, H-bond accepting base; L_3 denotes interacting ligand with DNA base or with ammonium; and L_4 means second water or ammine group in trans position to first base.

Table 2. H-bond Parameters in Pt−Base(s) Complexes

species	H···X_6	L^a−H(···X_6)
Pt_a_2wA	1.563	1.062
Pt_a_3A	2.024	1.041
Pt_a_2wG	1.450	1.057
Pt_a_3G	1.799	1.043
Pt_a_2A_2(s)	2.050	1.038
Pt_a_2A_2: L···B_d[b]	2.119	1.038
Pt_a_2A_2: B_d···B_a	2.280	1.024
Pt_a_2AG: L···B_d	2.087	1.038
Pt_a_2AG: B_d···B_a	2.012	1.024
Pt_a_2G_2	1.840	1.039

[a] L means O atom in water or N atom in ammine ligand L_3 (in Scheme 1). [b] B_d and B_a label the base which donates/accepts a proton in the interbase H-bonding.

structures were already analyzed elsewhere,[23] this part is reduced substantially.

Comparing single-base complexes and small complexes, the trans Pt−N(ammine−L_4) bonds vary under the influence of different ligands. The longest Pt−L_4 bond occurs in the presence of adenine (about 2.117 Å), and the shortest bond in the presence of water (about 2.055 Å). This is indicative of the strength of the trans effect of the coordinated ligands (H_2O < NH_3 < guanine ≤ adenine). The last inequality seems to be surprising since the Pt−N_7 bond with guanine is stronger than the corresponding bond with adenine (compare, e.g., the BDEs in Table 4). Nevertheless, the strength of the Pt−N_7 bond is influenced by the non-negligible Coulombic portion of the interaction energy of the Pt−DNA base interaction. Also, the stronger intramolecular H-bond between the ammonium ligand and the X_6 position of the base (cf., the shorter H···O_6 distances for guanine complexes in the first column of the upper part of Table 2) partially influences the Pt−N_7 bond. However, the Pt−N_7 bond distances are more transparent for comparisons of the trans effect. The Pt−N_7 (adenine) bond is in all comparable cases shorter than the Pt−N_7 (guanine) bond. Similar bond length trends were also observed in previous works.[28] According to theoretical considerations, ligand polarizability plays a key role in the trans effect. Comparing both DNA bases, their polarizability tensors are similar.

Table 3. Stabilization Energies of the Investigated Pt Complexes: Uncorrected, without BSSE Corrections, DFT/6-31G(d)[a]

species	ΔE^{uncor} (DFT)	ΔE^{uncor} (MP2)	ΔE^{stab} (MP2)	ΔE^{stab} (bsse + def)	ΔE^{stex} (MP2)
Pt_a_2w_2	447.7	431.5	404.0	403.7	19.2
Pt_a_3w	466.3	454.3	425.5	425.1	22.3
Pt_a_4	485.7	478.2	449.5	449.0	25.4
Pt_a_2wA	489.4	482.9	462.6	453.7	22.8
Pt_a_3A	501.6	500.2	473.2	467.8	20.0
Pt_a_2wG	515.3	503.5	479.6	470.8	25.5
Pt_a_3G	526.7	520.9	493.5	488.9	22.4
Pt_a_2A_2(s)	508.9	516.3	489.7	480.4	25.0
Pt_a_2A_2	509.1	519.0	491.5	482.1	15.8
Pt_a_2AG	536.2	542.8	514.6	506.7	16.5
Pt_a_2G_2	555.1	555.3	528.3	524.4	28.7

[a] Superscript stab and stex are defined in text, in kcal/mol.

(43) Frisch, M. J.; Trucks, G. W.; Schlegel, H. B.; Scuseria, G. E.; Robb, M. A.; Cheeseman, J. R.; Zakrzewski, V. G.; Montgomery, J. A., Jr.; Stratmann, R. E.; Burant, J. C.; Dapprich, S.; Millam, J. M.; Daniels, A. D.; Kudin, K. N.; Strain, M. C.; Farkas, O.; Tomasi, J.; Barone, V.; Cossi, M.; Cammi, R.; Mennucci, B.; Pomelli, C.; Adamo, C.; Clifford, S.; Ochterski, J.; Petersson, G. A.; Ayala, P. Y.; Cui, Q.; Morokuma, K.; Malick, D. K.; Rabuck, A. D.; Raghavachari, K.; Foresman, J. B.; Cioslowski, J.; Ortiz, J. V.; Stefanov, B. B.; Liu, G.; Liashenko, A.; Piskorz, P.; Komaromi, I.; Gomperts, R.; Martin, R. L.; Fox, D. J.; Keith, T.; Al-Laham, M. A.; Peng, C. Y.; Nanayakkara, A.; Gonzalez, C.; Challacombe, M.; Gill, P. M. W.; Johnson, B. G.; Chen, W.; Wong, M. W.; Andres, J. L.; Head-Gordon, M.; Replogle, E. S.; Pople, J. A. *Gaussian 98*, revision A.1x; Gaussian, Inc.: Pittsburgh, PA, 2001.

Table 4. Bond Dissociation Energies (BDEs) in kcal/mol

species	bond type	ΔE (MP2)
Pt_a_2w_2	Pt−NH_3	94.6
	Pt−H_2O	54.2
Pt_a_3w	Pt−NH_3_L_1	81.5
	Pt−NH_3_L_2	89.6
	Pt−NH_3_L_4	78.1
	Pt−H_2O	53.3
Pt_a_4	Pt−NH_3	77.7
Pt_a_2wA	Pt−NH_3_L_2	79.5
	Pt−NH_3_L_4	75.8
	Pt−H_2O	63.6
	Pt−adenine	114.1
Pt_a_3A	Pt−NH_3_L_2	71.8
	Pt−NH_3_L_3	79.2
	Pt−NH_3_L_4	72.1
	Pt−adenine	101.8
Pt_a_2wG	Pt−NH_3_L_2	76.8
	Pt−NH_3_L_4	75.2
	Pt−H_2O	63.3
	Pt−guanine	131.8
Pt_a_3G	Pt−NH_3_L_2	68.6
	Pt−NH_3_L_3	78.6
	Pt−NH_3_L_4	71.1
	Pt−guanine	122.2
Pt_a_2A_2(s)	Pt−NH_3	74.7
	Pt−adenine	89.9
Pt_a_2A_2	Pt−NH_3_L_3	74.3
	Pt−NH_3_L_4	69.3
	Pt−Ade•(do)	97.4
	Pt−Ade•(ac)	89.7
Pt_a_2AG	Pt−NH_3_L_3	73.0
	Pt−NH_3_L_4	68.2
	Pt−adenine	94.9
	Pt−guanine	112.4
Pt_a_2G_2	Pt−NH_3	72.8
	Pt−guanine	103.2

However, the orientation of the ellipsoid axes is slightly more preferable in the case of adenine. This is in contrast to the dipole moment vectors. In the case of Pt(II)−N_7 guanine interactions, the dipole moment is larger and more favorably oriented than for the adenine complex.

The length of the Pt−N (ammine) bond in the cis interacting L_3 position corresponds to the strength of the intramolecular H-bond in these complexes. The guanine O_6 atom creates the strongest H-bond with the neighboring aqua/ammine ligand, making the bond relatively shorter. The outer cis Pt−N (L_2 ammine) bond can be considered as a result of both effects: trans and H-bonding. In the case of ligands with approximately equal trans effect (guanine and adenine), the stronger H-bond leads to a longer Pt−N distance of outer cis-ammonia bond (about 2.111 Å).

In the case of Pt_a_2wB, several conformers were found, most of them characterized by relative energies within 5 kcal/mol from the global minimum. The most stable structures used for further analyses and discussion are shown in Figure 1a,b, together with the ligand notation for clarity. The Pt−O bond in single base complexes (Pt_a_2wB) displays the same behavior as the Pt−N (L_3 ammine) bonds. A shorter Pt−O bond occurs in guanine-containing complexes due to a stronger H-bridge O_6···H, which reduces the H−O (water) bond electron density resulting in a stronger Pt−O interaction. It is interesting that the Pt−O length is even shorter than any Pt−N (ammine) distances in both Pt_a_2wA and Pt_a_2wG.

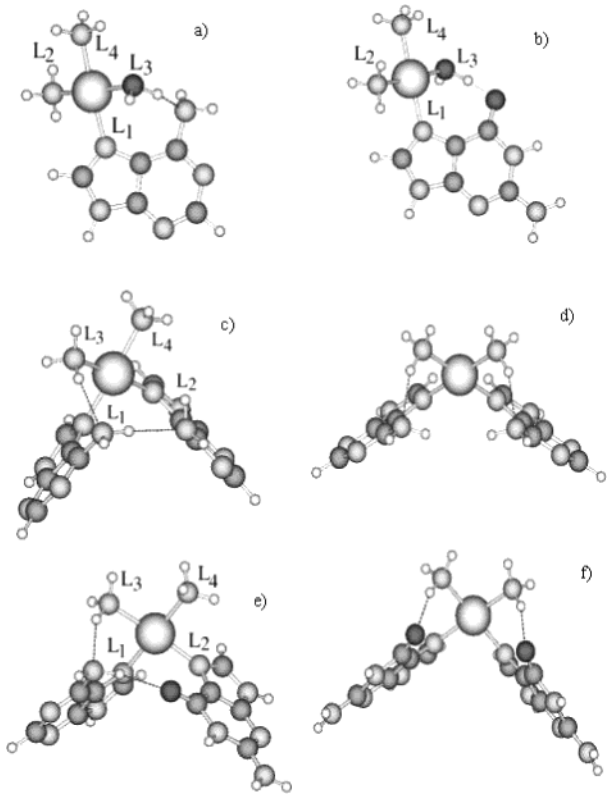

Figure 1. Optimized structures of selected Pt complexes together with ligand notation: (a) Pt_a_2wA, (b) Pt_a_2wG, (c) Pt_a_2A_2, (d) Pt_a_2A_2(s), (e) Pt_a_2AG, and (f) Pt_a_2G_2.

In the case of two DNA bases bridged by the Pt atom, two stable structures were found for the bi-adenine complex (cf. Figure 1c,d). The symmetrical complex Pt_a_2A_2_s has a C_s point group with two equivalent (ammine)N−H···N_6 intramolecular H-bonds. The nonsymmetrical complex is energetically slightly more preferable (by less than 1 kcal/mol at the Becke 3LYP level). This structure has also two H-bonds; both of them involve the same N_6 site of L_1 adenine. In the first case, this adenine accepts hydrogen from ammonium ligand L_3, and in the second case, it donates hydrogen from the ammine group to the other L_2 adenine. Comparing the Pt−N distances in both complexes, a distinct shortening of the Pt−N_7 bonds can be seen together with a enlargement of the Pt−N (ammine) bonds in the nonsymmetrical complex. To some extent, these bi-adenine structures can be considered as weaker forms of both types of Pt-bridged structures found here: in bi-guanine Pt_a_2G_2 (symmetrical) and in mixed Pt_a_2AG complexes. In the mixed AG complex (in Figure 1e), two H-bonds exist, both based on the adenine L_1 amino group: (1) interbase HN_6−H···O_6 where adenine is an H-donor and (2) H_2N−H···N_6 where adenine accepts a proton from the ammonium ligand L_3. The bi-guanine C_s structure is stabilized by two strong H_2N−H···O_6 H-bridges (cf. Figure 1f).

The shortest Pt−NH_3 bond occurs in the complex with two guanine bases, followed by the Pt−NH_3 bond from the mixed Pt_a_2AG system, and then from the bi-adenine complex. The Pt−N_7 bonds show a different trend. The shortest bond occurs in the Pt_a_2AG complex. This could be slightly surprising because the value of this bond length

in the mixed system should be expected somewhere between those for pure bi-adenine and bi-guanine complexes, similarly to Pt−NH_3 bonds. However, the reason can be explained by the sterically more advantageous orientation of the bases in a nonsymmetrical arrangement. The symmetrical minimum of the bi-guanine complex exhibits a slightly larger N_7−Pt−N_7 angle, with a value of 93.4° (94.5° for the bi-adenine complex). Also, the C_8 hydrogen atoms are located close to each other (about 2.4 Å in bi-guanine and 2.3 Å in the bi-adenine complex). On the other hand, the mixed Pt_a_2AG and nonsymmetrical bi-adenine complexes with one interbase H-bond possess a structure where the N_7−Pt−N_7 angle is practically rectangular (about 91°), and the interatomic distance between the hydrogens on C_8 is approximately 3.2 Å. In this way, the Pt−N_7 bonds are not significantly influenced by steric tension, which leads to shorter bonds (less than 2.05 Å). The Pt−NH_3 bonds are prolonged, accordingly. The striking feature can be seen in the last column where the torsion angle (ammine-ligand) N−Pt−N_7−C_5 is given. Large values of torsion angle for Pt_a_2AG (94°) and Pt_a_2A_2 (107°) correspond to a partial shift of the bases in the platinum bridged complexes causing some steric relaxation.

Selected data concerning intramolecular H-bonds are collected in Table 2. From the first column, shorter H-bonds in the case of guanine are remarkable. Even the interbase H-bond (guanine)O_6···H(NH)(adenine) in the mixed Pt_a_2-AG complex is relatively short, making the asymmetry of the mixed complex more pronounced. In the next column of Table 2, the O−H and N−H distances are compiled. In the lower part of Table 2, it can be seen that shorter N−H bonds in the NH_2 amino group of adenine generally are indicative of stronger bonds in adenine than in ammonia ligands (cf. IR spectra of adenine-containing complexes for another insight).

Optimized geometries were compared with the crystal structures found in the NDB database (http://ndbserver.rutgers.edu/NDB/structure-finder/ndb/index.html) where Pt structures coordinated to both one and two guanines can be found.[3−8] From Table 2, longer Pt−N_7 distances can be seen for complexes with a single guanine (ddl017 or zdfb42), but in these cases, the lower resolution can play an important role. For instance, in the ddl017 structure,[3] three different Pt−N_7 distances are present in the 0.2 Å range. Substantially shorter distances were obtained in the cases of Pt links to two guanines. Here, the agreement with our results is better (within 0.1 Å). Also, Pt−N_7 bonds are on average slightly longer than Pt−N(ammine). Experimental N_7−Pt−N_7 angles are somehow larger than the optimized ones by about 5°. The differences in torsion angle N(ammine)−Pt−N_7−C_5 are due to the symmetrical model of Pt_a_2G_2 (without sugar−phosphate backbone).

Stabilization and Ligand-Substitution Reactions of the Complexes. The complex stabilization energies are collected in Table 3. Starting from Pt compounds containing small complexes, it can be noticed that the replacement of ammonium with water causes a decrease in the stability of the complex by about 20 kcal/mol at both the MP2 and DFT levels. This fact was already discussed at various levels of theory by many researchers (e.g., refs 23, 26, 30, 44). The BDE of Pt−NH_3 (Table 4) also changes but in the opposite direction: from 78 kcal/mol for Pt_a_4 through 83 kcal/mol (Pt_a_3w) to 95 kcal/mol for Pt_a_2w_2. This clearly shows a rearrangement of electron density distribution at the expense of water donation. From Table 3, column E^{stex}, sterical energy corrections, it can be seen that the lower affinity of oxygen to Pt is partially compensated by the lower ligand repulsion in aqua-complexes (by about 3 kcal/mol).

All considered complexes become more stable after base substitution. The stability increase correlates with larger values of the base BDE (cf. Table 4). The BDE of Pt−N_7 adenine is about 30 kcal/mol larger than the BDE of Pt−NH_3, and the analogous difference for guanine-containing compounds is roughly 50 kcal/mol, i.e., practically twice as much as the BDE of Pt−ammonium. As mentioned in previous papers,[28,29] adenine is more weakly bound to Pt(II) than guanine. The difference depends on the total charge of the system, and it amounts to about 20 kcal/mol for 2+ charged complexes. Clearly, the donating ability of both DNA bases is higher than that of either water or ammonia. In complexes with water, the larger increase of the Pt−base BDE (about 10 kcal/mol) is connected with the smaller binding energy of Pt−water. This leads to the rearrangement of electron distribution so that the BDE of Pt−ammonium remains practically unchanged. Nevertheless, an interesting detail here concerns the noninteracting ligand L_2 where an increase of the Pt−ammonium BDE is seen (about 8 kcal/mol). This correlates with the fact that these ammonias are in a trans position to water, which has a smaller trans effect, and thus, some secondary BDE strengthening can occur. Nevertheless, comparing the Pt−O BDE of small complexes (either Pt_a_3w or Pt_a_2w_2) with aqua single-base complexes (Pt_a_2wB), higher BDE (about 10 kcal/mol) can be observed in the presence of the base. This points to some basic difference in the DNA base coordination to the Pt atom, which can be recognized in the back-donation ability of the base. Both the aqua complexes (Pt_a_2wB) are less stable than the corresponding Pt_a_3B species, but the difference is reduced to one-half (about 10 kcal/mol) of a similar difference between the stabilization energies of small complexes. Smaller ligand repulsion (ΔE^{stex}) in the case of adenine complexes is a consequence of its smaller dipole moment, in comparison with guanine.

When the second base replaces the ligand in the L_2 position, the Pt-bridged structure is formed. The stabilization energy is again increased by about 15−30 kcal/mol, depending on the base. Strong donating competition is observed in all of these Pt-bridged complexes. It leads to a decrease in the BDE of Pt−adenine from 100 to 90 kcal/mol and of the corresponding Pt−guanine value from 120 to 100 and 110 kcal/mol for Pt_a_2G_2 and Pt_a_2AG, respectively. The smaller decrease in the BDE of guanine in the mixed Pt_a_2AG complex is partially compensated by the small BDE of Pt−ammonium, especially in the noninteracting L_4 position. This

(44) Burda, J. V.; Zeizinger, M.; Leszczynski, J. In preparation.

Table 5. Reaction Energies for Ligand Substitution (in kcal/mol)

	MP2/6-31+G(d)		Becke 3LYP/6-31G(d)	
	L = NH_3	L = H_2O	L = NH_3	L = H_2O
$B + Pt(NH_3)_2LL' \rightarrow L' + Pt(NH_3)LB$				
B = adenine	−22.0	−51.4	−15.91	−41.68
B = guanine	−42.7	−72.0	−40.99	−67.57
$B1 + Pt(NH_3)LB2 \rightarrow L + Pt(NH_3)_2B_1B_2$				
B_1 = A; B_2 = A	−16.1	−33.4	−7.29	−19.52
B_1 = A; B_2 = G	−21.8	−39.2	−9.47	−20.89
B_1 = G; B_2 = A	−42.5	−59.8	−34.56	−46.78
B_1 = G; B_2 = G	−34.3	−51.7	−28.37	−39.79
Total: $B_1 + B_2 + Pt(NH_3)_2L_2 \rightarrow 2L + Pt(NH_3)_2B_1B_2$				
B_1 = A; B_2 = A	−38.1	−84.8	−23.20	−61.20
B_1 = A; B_2 = G or B_1 = G; B_2 = A	−64.6	−111.3	−50.46	−88.46
B_1 = G; B_2 = G	−77.1	−123.8	−69.36	−107.36

BDE represents the lowest value from the whole set of Pt-ammonium binding energies. Simultaneously, the more favorable structural arrangement of the Pt_a_2AG complex leads to the largest BDE for both adenine and guanine among the Pt-bridged complexes. Steric repulsion is the lowest for the asymmetrical Pt-bridged complexes from the whole set of examined systems, about 16 kcal/mol. The only larger stabilization is exhibited by the Pt_a_2G_2 complex. The substantially stronger electrostatic contributions of Pt_a_2G_2 are partially reduced by sterical repulsion (about 29 kcal/mol), which is, on the contrary to Pt_a_2AG, the largest from the whole set.

It should be noticed that the BDE of Pt−ammonium is fairly constant (about 74 kcal/mol) with only a few exceptions. The largest negative deviation represents the BDE of the Pt−NH_3 bond in the Pt_a_2AG complex (below 69 kcal/mol) where ammonium is in the trans (L_4) position to adenine. The largest positive BDE deviation occurs in Pt_a_3w for Pt−L_2 in the trans position to water (above 89 kcal/mol). This means that both extremes are related to the trans effect.

Comparing the stabilization energies obtained from the DFT approach with MP2 methods, DFT underestimates the stabilization energies for bridged complexes up to 10 kcal/mol. However, approximately the same overestimation can be observed for the single-base complexes. A relatively worse agreement was obtained for small complexes (a difference in energies up to 16 kcal/mol).

Besides the stabilization energies and BDEs, the reaction energies (RE) for ligand substitution were also evaluated. In Table 5, the effect of replacement of water or ammonia with a base is depicted. At first glance, it is seen that all of these reactions are exothermic. Comparing columns for ammonia and water substitution, one can notice that the substitution of the first water is facilitated by approximately 30 kcal/mol and the second water by approximately 15−20 kcal/mol. This fact correlates closely with the higher stabilization of the ammine complexes over the aqua complexes. It is interesting to mention that the ligand replacement with the second base is energetically not so efficient. The only exception is ammine-ligand substitution by a different base, thus creating the mixed Pt_a_2AG complex. A possible explanation concerns the better structural rearrangement, which minimizes the repulsion forces. The stronger intermolecular H-bonds make this reaction more feasible, too. Similarly, aqua-ligand replacement is also more facilitated (about 6−8 kcal/mol) in this case. Then, the REs of Pt_a_2AG are much closer to those of the Pt_a_2G_2 complex than to those of the Pt_a_2A_2 complex. In the last two columns of Table 5, values of RE obtained with the DFT technique are present. Contrary to the differences between DFT and MP2 results for the BDE estimations, all of the REs are systematically lower using the DFT method here.

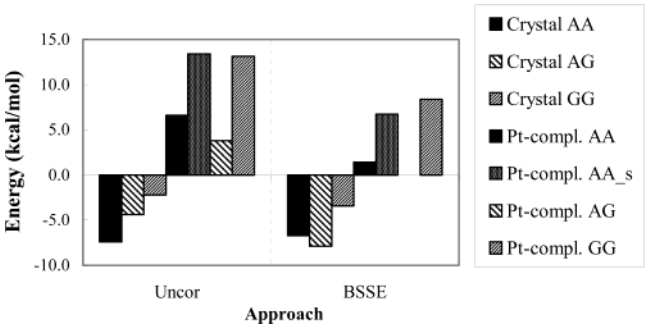

Figure 2. Comparison of the stacking energies for geometries taken from crystallographic data and Pt bridged structures; uncor indicates uncorrected approach, BSSE indicates inclusion of BSSE corrections.

Table 6. Base Stack Interactions for Selected Crystal Structures and Pt-Bridged Complexes (in kcal/mol)

crystal	ΔE^{uncor}	ΔE^{BSSE}
AA cryst	−7.4	−6.7
AG cryst	−4.4	−7.9
GG cryst	−2.2	−3.4
Pt_a_2A_2(s)	13.4	6.7
Pt_a_2A_2	6.6	1.4
Pt_a_2AG	3.8	0.0
Pt_a_2G_2	13.2	8.4

Since the Pt-bridges perturb the ordered structure of DNA bases, it is important to know to which extent such perturbation affects the stacking energies. Therefore, a comparison with the stacked structures was performed. It is known[45] that the stacking interaction is much weaker than H-bonding between the base pairs. On the basis of MP2 calculations, Šponer et al. showed that the largest stacking energy is for G···G bases, about 11 kcal/mol for the partially optimized structures (using empirical potential calculation). The A···G bases exhibit practically the same stacking energy. The stacking energy of A···A bases is about 9 kcal/mol. Our results concern randomly chosen crystal structures taken from the NDB database, just for illustration of the particular phenomenon treated in a consistent way. Using the same method and basis set, the relation between the stacked bases and bridged bases can be compared. From Table 6 and Figure 2, it is evident that the stacking interaction is present in all three examples taken from crystal structures. These values are not so high as for optimized structures from Šponer's work. Nevertheless, for A···A bases, the estimation of stacking energy is fairly close to their results (about 7 kcal/mol). The stacking energy of the GG bases is relatively smaller (slightly above 3 kcal/mol). However, the stacking interactions remain attractive in all of these cases. Regarding bridged complexes, the character of the interaction is changed

(45) Šponer, J.; Leszczynski, J.; Hobza, P. *J. Phys. Chem.* **1996**, *100*, 5590−5596.

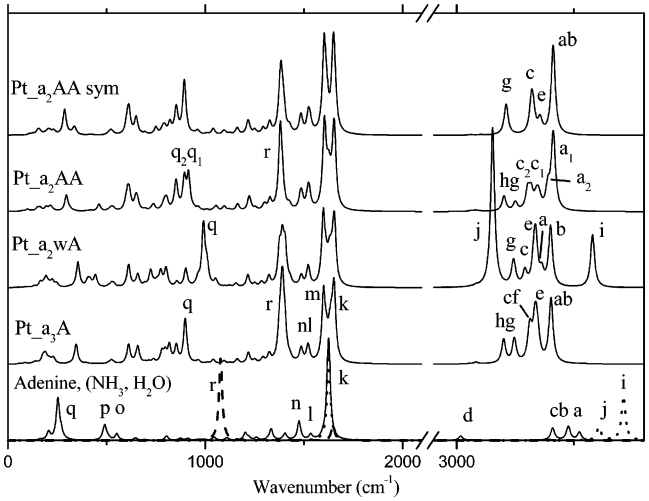

Figure 3. Calculated IR spectra for adenine-containing complexes at HF/6-31G(d) level.

to moderate repulsion, especially for symmetrical complexes. This is due to the mutual orientation of dipole moments. The straightforward consequence leads to the conclusion that the symmetrical structures exhibit the largest repulsion. Moreover, some additional attraction, caused by the interbase H-bond between donating adenine and the second base, diminishes the resulting repulsion in both nonsymmetrical Pt-bridged complexes. The repulsion vanishes completely for the Pt_a$_2$AG complex within the BSSE approach.

IR Spectra. For a deeper understanding of Pt(II) interactions with bases and the influence of intramolecular H-bonds on electronic properties, vibration spectra analyses were performed. The obtained spectral line and intensities were interleaved with Lorentzian peaks at a temperature of 298 K.

Figure 3 contains IR spectra of isolated adenine, ammonia, and water (bottom curves), followed by the spectrum of the Pt_a$_3$A complex, Pt_a$_2$wA, and, at the top, two spectra of the bridged Pt_a$_2$A$_2$ complexes with and without symmetry.

Three small peaks around 3500 cm^{-1} belong to the antisymmetrical stretch of NH_2 (3520 cm^{-1}, a in Figure 3), N_9-H (3480 cm^{-1}, b), and symmetrical stretch of the NH_2 group (3410 cm^{-1}, c). In the middle part, the dominant peak (1620 cm^{-1}) represents the NH_2 in-plane bend mode (k) with some small admixture of adenine deformation and other modes. In the very end of the adenine spectrum, there is a symmetrical out-of-plane bending of the NH_2 group (250 cm^{-1}) (q). The bending modes of both water and ammonia are above 1600 cm^{-1} (coincidence with k peak), and the umbrella vibration of NH_3 (r) is remarkable at 1000 cm^{-1}.

Moving from isolated molecules to the Pt complexes, the energy shift of individual modes gives some quantitative measure of the strength of intramolecular interactions. In Pt_a$_3$A, both the N_9-H and asymmetric NH_2 stretches are shifted to lower frequencies (3400 cm^{-1}) and are practically degenerated. From this particular point, it can be seen that adenine electron density is polarized due to the Pt adduct. This is connected to the weakening of both N_9-H and N_6-H bonds and to the decreased frequencies of the stretch modes. Furthermore, the weakening is more remarkable for the NH_2 group since additional H-bonding interactions with one of the ammonia ligands (L_3) takes place. The change in the NH_2 asymmetric stretch is as follows: 3524 cm^{-1} (isolated adenine), 3418 cm^{-1} (Pt_a$_2$A$_2$(s)), 3399 cm^{-1} (Pt_a$_3$A), 3398 cm^{-1} (Pt_a$_2$AG), 3406 cm^{-1}, 3389 cm^{-1} (Pt_a$_2$A$_2$), and 3365 cm^{-1} (Pt_a$_2$wA). From the series, it follows that the strongest H-bond occurs in the Pt_a$_2$wA complex. Moreover, the NH_2 mode is the highest energy peak only in the case of isolated adenine and Pt_a$_2$A$_2$(s). The N_9-H stretch has a higher frequency for the other species. Inactive ammonia modes in the isolated molecule become visible here; their shift is about 60 cm^{-1} for asymmetric modes (e). Moreover, one of the asymmetric modes, which belongs to the interacting (L_3) NH_3, lies at a slightly lower frequency (3310 cm^{-1}, f) and is degenerate with the symmetric stretch of the NH_2 group of adenine (c). Similarly, the symmetrical mode of L_3 ammonia is influenced by H-bonding and is split into two peaks: for the L_2 and L_4 ligands at 3250 cm^{-1} (g) and for the L_3 ligand 3200 cm^{-1} (h). In the middle range, it is noteworthy to mention the three highest peaks. The twin peaks (1650 and 1600 cm^{-1}) have dominant contributions from the NH_2 bending mode (k) and the C_2-H in-plane bend (m). The other peak (1390 cm^{-1}) is composed of all three umbrella modes of the NH_3 ligands (r). This mode from the isolated NH_3 molecule (dotted line below) is about 1070 cm^{-1}. Its blue shift is caused by increased Coulombic repulsion between the positively charged hydrogen and the Pt ion. A shift of the out-of-plane mode of the NH_2 adenine group is even more pronounced (to 900 cm^{-1}, q) and can be explained by the formation of the intramolecular H-bond with the L_3 ammonium ligand.

Pt_a$_2$wA exhibits similar trends as those observed in previous IR spectra. In the range above 3000 cm^{-1}, new features appear. Peaks belonging to the O−H vibrations frame this band range. Both peaks are at a lower frequency than the original water vibrations for antisymmetrical and symmetrical modes. The higher (3580 cm^{-1}), less intensive peak belongs to the noninteracting O−H bond (i). The most dominant peak from the whole spectrum (3150, j) is related to the other O−H bond, which has a substantially smaller frequency due to the relatively strong H-bond at the N_6 site of adenine. The red shift of the NH_2 peaks (a) clearly corresponds to a stronger H-bond in the aqua-complex. The same conclusion can be drawn from larger blue shift of the out-of-plane bend mode for the NH_2 group (990 cm^{-1}, q).

IR spectra of guanine-containing complexes are collected in Figure 4. In the range above 3000 cm^{-1}, a mild blue shift (only about 20 cm^{-1} higher in comparison with the spectrum of isolated guanine) of both the antisymmetrical (a) and symmetrical (c) stretch vibrations of the NH_2 groups can be noticed in Pt_a$_3$G spectra. The other X−H stretch modes, b and d−j exhibit a red shift which can be explained in the same way as in the cases of adenine (also labels have the same meaning as in adenine-containing complexes; only d denotes N_1-H stretch mode). Similarities to Pt_a$_2$wA can be observed in this region for the Pt_a$_2$wG complex, too. One antisymmetrical (e) and symmetrical (g) NH_3 modes

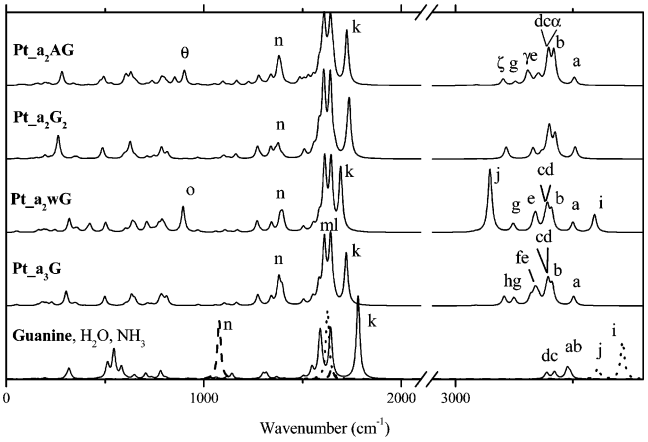

Figure 4. Calculated IR spectra for Pt-complexes with guanine.

and the O−H modes i and j are present here. An interesting case represents the spectrum of mixed Pt_a$_2$AG species. Besides guanine lines, adenine modes are visible, too. These modes are labeled in Greek: α, β, and γ correspond to a, b, and c in the adenine spectra. ζ is an analogue to the g mode associated with the L_4 ligand.

In the middle spectra parts, the most intensive peak belongs to the guanine C═O vibration (k). The shift of this vibration corresponds to the strength of the intramolecular H-bond. It can be used as a measure of the H-bond interaction in analogy to the NH_2 asymmetric stretching mode in the adenine systems. The values are 1780 (isolated guanine), 1740(Pt_a$_2$G$_2$), 1720 (Pt_a$_3$G), 1690 (Pt_a$_2$wG), and 1641-(Pt_a$_2$AG) cm^{-1}. This means that the Pt_a$_2$AG complex has the strongest H-bond. The symmetrical Pt-bridged guanine complex has the weakest H-bonds. It should be stated that, besides H-bonding to O_6 site, the frequency of the C═O bond can also be influenced by Pt−N_7 coordination the through a polarization effect, too. The other intensive twin peaks originate from the in-plane bends of the NH_2 group (l) and the N_9−H bond (m). The umbrella modes of the ammonia ligands (n) are also substantially blue-shifted when the base is platinated. The explanation follows the arguments mentioned in the discussion of adenine r peaks. An extra peak θ corresponds to the out-of-plane mode of the NH_2 group of adenine. A similar peak in the Pt_a$_2$wG spectra is connected with the O−H out-of-plane mode (o).

Wave Function Analyses and Charge Distributions. Partial charges of Pt and the closest ligand atoms are summarized in Table 7. Atom ordering is depicted in Scheme 1. From the first column of the Pt charges, it can be noticed that the most positive value occurs in the complex with two water ligands. This implicates the oxygen atom as having less ability to donate a nonbonding electron pair to platinum and, thereby, weaker affinity to such a type of metal. It is also known that water and ammonium have minimal ability for accepting back-donation.[46] In accord with the trans effect, lower partial charges on Pt systematically occur in adenine complexes in comparison with guanine complexes. This demonstrates the better donation ability of adenine over guanine. Electron density of N (ammonium) is generally lower in the L_3 position of the interacting ligands. The exceptions are the nonsymmetrical bridged complexes Pt_a$_2$A$_2$ and Pt_a$_2$AG where the ammonium nitrogen at the interaction site is slightly less negative. In the presence of ligated water, the electron density of the N atom is lower, especially in the trans position to oxygen (L_2-site). This can be explained by the higher donation of electron density to the Pt atom.

(46) Bersuker, I. B. *Electronic Structure and Properties of Transition Metal Compounds*; Wiley-Interscience: New York, 1996.

Table 7. Partial Charge Distributions Based on NBO Population on Pt and the Closest Ligand Atoms (N/O) (in eV)[a]

species	Pt	L_1		L_2		L_3		L_4	
Pt_a$_2$w$_2$	0.810	a	−1.025	a	−1.025	w	−0.968	w	−0.968
Pt_a$_3$w	0.749	a	−1.066	a	−1.026	w	−0.966	a	−1.072
Pt_a$_4$	0.676	a	−1.068	a	−1.068	a	−1.068	a	−1.068
Pta_a$_2$wA	0.733	A	−0.515	a	−1.044	w	−0.965	a	−1.061
Pt_a$_3$A	0.668	A	−0.513	a	−1.067	a	−1.061	a	−1.070
Pt_a$_2$wG	0.742	G	−0.492	a	−1.047	w	−0.957	a	−1.059
Pt_a$_3$G	0.682	G	−0.489	a	−1.070	a	−1.056	a	−1.067
Pt_a$_2$A$_2$(s)	0.661	A	−0.504	A	−0.504	a	−1.058	a	−1.058
Pt_a$_2$A$_2$	0.663	A	−0.479	A	−0.508	a	−1.064	a	−1.061
Pt_a$_2$AG	0.675	A	−0.494	G	−0.484	a	−1.063	a	−1.056
Pt_a$_2$G$_2$	0.684	G	−0.484	G	−0.484	a	−1.051	a	−1.051

[a] For ligand notation, see Scheme 1. Partial charges mentioned atoms from isolated molecules: $\delta^N(NH_3) = -1.156$e, $\delta^O(H_2O) = -0.990$e, δ^{N7}(guanine) $= -0.447$, and δ^{N7}(adenine) $= -0.488$e.

Table 8. NBO Partial Charges of DNA Bases

species	N_1	N_2^G/C_2^A	N_3	O_6^G/N_6^A	C_8	N_9
Pt_a$_3$A	−0.428	0.251	−0.400	−0.924	0.244	−0.516
Pta_a$_2$wA	−0.445	0.251	−0.418	−0.908	0.234	−0.515
Pt_a$_3$G	−0.611	−0.802	−0.522	−0.637	0.222	−0.525
Pt_a$_2$wG	−0.627	−0.808	−0.535	−0.619	0.212	−0.525
Pt_a$_2$A$_2$(s)	−0.457	0.247	−0.422	−0.894	0.245	−0.521
Pt_a$_2$A2: B$_a$	−0.462	0.246	−0.428	−0.880	0.231	−0.523
Pt_a$_2$A2: B$_d$	−0.459	0.245	−0.427	−0.907	0.242	−0.522
Pt_a$_2$AG: B$_a$	−0.634	−0.813	−0.539	−0.623	0.213	−0.531
Pt_a$_2$AG: B$_d$	−0.466	0.241	−0.434	−0.902	0.244	−0.527
Pt_a$_2$G$_2$	−0.632	−0.817	−0.541	−0.612	0.224	−0.532
isol. adenine	−0.527	0.210	−0.499	−0.842	0.202	−0.580
isol. guanine	−0.662	−0.874	−0.563	−0.571	0.181	−0.573

Table 8 contains partial charges on several important sites of the bases. Notice the pronounced polarization effect. All of the atoms exhibit a decrease in electron density: more positive or less negative partial charges after platination. The only exceptions are the atoms at the 6th and 7th position of the base in the closest neighborhood of Pt(II). An interesting feature can be seen from Table 7. While partial charges of O (water) and N (ammonium) are decreased in comparison with isolated molecules, the charges of the N_7 base sites are increased in the Pt complexes. An explanation involves the strong back-donation of the d_π-electrons from Pt. Such a donation is not possible towards water and ammonium.

These considerations can be confirmed with MO analyses. In all the complexes, an occupied MO can be found where "vacant" $5d_{x^2-y^2}$ Pt AO is admixed (with a coefficient of more than 0.30) in an orbital which contains electron lone pairs of the ligands. Another support of this orbital interaction can be seen in the fact that the LUMO contains 6s AO and the $5d_{x^2-y^2}$ orbital lies higher (with the antibonding contribution of the ligand electron lone pairs). In Figure 5a−d, the 22nd and 33rd MO of Pt_a$_4$ and the 22nd and 30th MO of Pt_a$_2$w$_2$ are displayed. Both complexes have 28 occupied MOs. From the differences between Figure 5a and c, one can notice a

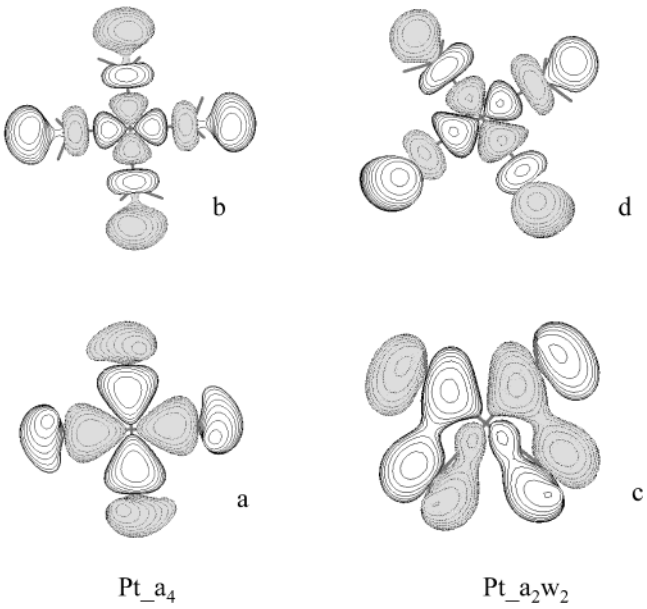

Figure 5. Molecular orbitals with the donation character: (a) Pt_a_4 complex, 22nd MO contains bonding combination of "vacant" Pt $5d_{x^2-y^2}$ AO and nitrogen p_z AOs with lone electron pairs from all NH_3 ligands; (b) Pt_a_4 complex, 33rd MO with antibonding combination of Pt $5d_{x^2-y^2}$ and all four N p_z AOs; (c) Pt_a_2w_2 complex, 22nd MO with bonding combination of Pt $5d_{x^2-y^2}$ AO and nitrogen p_z AOs + oxygen p_z AOs; d) Pt_a_2w_2 complex, 30th MO with antibonding combination of Pt $5d_{x^2-y^2}$ AO and nitrogen p_z AOs + oxygen p_z AOs.

(possibly general) explanation for the lower affinity of oxygen to the transition metal cations than nitrogen. While a single lone pair of p_z(N) of NH_3 is oriented in the Pt−N line, two lone pairs of oxygen are not appropriately oriented: the tetrahedral angle of 109° (suitable for dative bond) would cause too high a repulsion between positively charged hydrogens of water and the Pt atom. This leads to a larger (than 109°) angular position of water so the repulsion would be decreased, but simultaneously, the overlap between the water lone pair and the appropriate virtual AO of platinum is lowered, too. This leads to a weaker donor−acceptor interaction. No bonding combination corresponding to back-donation was found in these small complexes.

A much more complicated situation can be observed in complexes with one or two bases. Besides the already mentioned MO with a donation to Pt, the occupied orbital with a back-donation can be revealed. Figure 6a,b shows the 81st MO of Pt_a_2G_2 and the 77th MO of Pt_a_2AG where the antibonding π^* orbital of guanine (vacant in isolated molecule) creates a bonding combination with the d_{xy} AO of Pt. The MO with back-donation lies higher in energy than the MO with donating features. Figure 6c depicts a rare direct covalent interaction of Pt with the O_6 site in the 79th MO of Pt_a_2AG.

Conclusions

This study reveals properties and structures of Pt-bridged complexes of DNA purine bases coordinated to the Pt atom at the N_7 sites.

It was found that nonsymmetrical structures exist for Pt_a_2-AG and Pt_a_2A_2 complexes. Symmetrical complexes occur for Pt_a_2G_2 and Pt_a_2A_2, as a second slightly higher-lying

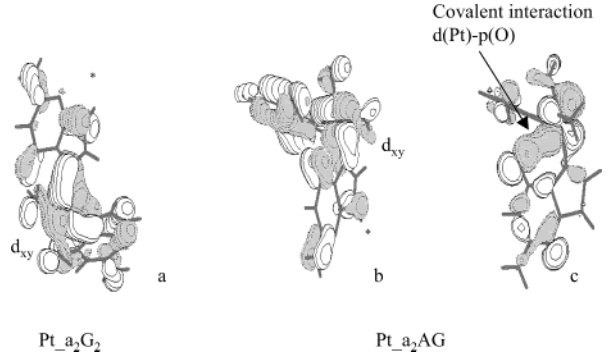

Figure 6. Back-donating character from Pt d_{xy} AO to antibonding π^* orbitals of guanine (vacant in isolated base): (a) 81st MO of Pt_a_2G_2, (b) 77th MO of Pt_a_2AG, and (c) rare form of covalent interaction between the Pt and O atoms.

(<1 kcal/mol) conformer. These models deviate from experimentally observed structures. Nevertheless, from newly obtained results, the bonding relations remain conserved in a more complete Pt-1,2-d(GpG) description.[47]

The influence of the trans effect of individual ligands is revealed. It is shown that the highest trans effect is exhibited by adenine, followed by guanine, ammonium, and water in accordance with their polarizability.

Energy analyses based on stabilization, BDEs, and REs for two-step replacement of small ligands with bases revealed that, besides the generally known fact concerning the stronger coordination of Pt-G over Pt-A, surprisingly the highest Pt affinity to guanine (BDE) occurs in the mixed Pt_a_2AG complex. This fact is only partially due to larger sterical repulsion in Pt_a_2G_2.

From the calculated Pt-bridged energies, it follows that the observed G−Pt−G bridges, responsible for the kink on DNA helix, are the strongest among the examined complexes. The second most stable Pt-bridge, A−Pt−G, is about 20 kcal/mol weaker, and thus, its occurrence in the helix must be very low (according to the Boltzmann relation for equilibrium between two states). Since the A−Pt−A structure is about another 20 kcal/mol less stable, it is practically impossible to find it even in nonequilibrated systems.

Cisplatin bridges are relatively very strong formations. Bond dissociation energies of Pt−guanine coordination are higher than 100 kcal/mol, and the BDE is about 90 kcal/mol for the Pt−adenine one. These energies seem to be sufficiently large for causing difficulties in some bio-operations (e.g., replication) occurring in the DNA helix.

It is shown that weak base stacking energy diminishes under complexation.

From the shifts of the corresponding vibrational modes, the strength of the intramolecular H-bond follows the following orders: Pt_a_2wA > Pt_a_2AG ≈ Pt_a_3A ≈ Pt_a_2A_2 for adenine complexes and Pt_a_2wG > Pt_a_2AG > Pt_a_3G > Pt_a_2G_2 for guanine. Both trends are largely similar.

The MO and NBO partial charge analyses explain bonding relations in terms of donating and back-donating abilities of individual ligands which are important for the explanation

(47) Burda, J. V.; Zeizinger, M.; Šponer, J.; Lezsczynski, J. In preparation.

of energy dependencies (stabilization energies, BDEs, and REs) from the perspective of wave functions.

Acknowledgment. This study was supported by Charles University Grant GAUK 181/2002/B_CH/MFF and the NSF-MŠMT CR ME-517 grant (J.V.B.). Partial support was also gained by the NSF Grant OSR-94527857 and by the Office of Naval Research, Grant N00014-95-1-0049. Special thanks should be given to the computational resources from MetaCentres in Prague, Brno, and Pilsen for excellent access to their supercomputer facilities and their kind understanding. The same applies to the Mississippi Supercomputing Research Center which supported us with a lot of CPU time. The program for drawing vibrational spectra was obtained from Dr. Petr Bouř from the Institute of Organical Chemistry and Biochemistry CAS in Prague.

IC034296W